

Aerodynamic Characteristics of a Three-Dimensional HLFC wing in Transonic Flow*

Yoji ISHIDA*¹

Masayoshi NOGUCHI *²

Koichi SUZUKI*³

ABSTRACT

We have made a transonic wind tunnel test of an HLFC wing model with a new leading edge suction system incorporated with a natural laminar flow airfoil to check mainly a drag reducing effect of the suction system in transonic Mach number range. The test has confirmed that the system works well on both design and off-design conditions: it can produce significant drag reduction in a wake drag with even small amount of suction quantity. Besides the drag reducing effect, it is found that the system produces considerable lift increase for some suction quantity range in wide range of test Mach number. The lift increment generates higher L/D value than that expected from only the drag reduction.

Keywords: Hybrid Laminar Flow Control, Drag reduction, Transonic flow

概 要

自然層流翼型に組み込んだ前縁吸い込みシステムを持つハイブリッド(HLFC)層流制御翼模型の、主に遷音速マッハ数における抵抗低減効果を確認するために、風洞試験を行なった。その結果本システムは設計、非設計条件の如何にかかわらず、きわめてわずかな吸い込みにより、大きなウエーク抵抗の減少を与えることが確認された。この抵抗低減効果のほかに本試験では、かなり広いマッハ数領域において、ある範囲の吸い込み量に対して揚力が吸い込み無しの時より増加することが見いだされた。この揚力の増加は、抵抗の低減だけから期待されるよりはるかに大きな揚抗比の増加をもたらす。

Nomenclature

c	local chord length
C_{DW}	section wake drag coefficient
C_{DB}	overall wing drag coefficient
C_L	overall wing lift coefficient
C_p	wing surface pressure coefficient
C_Q	suction flow quantity coefficient
C_{QDmin}	suction flow quantity coefficient at which C_{DB} becomes minimum
C_{QLmax}	suction flow quantity coefficient at which C_L becomes maximum
D	overall wing drag
L	overall wing lift

M_{DD}	drag divergence Mach number
M_∞	free stream Mach number
Q_T	total suction flow quantity, <i>litre/min</i>
U_∞	free stream velocity, <i>m/sec</i>
v_w	suction flow velocity, <i>m/sec</i>
x	streamwise ordinate
z	spanwise ordinate
α	angle of attack, <i>deg.</i>
ρ	flow density

subscript

w	model surface
∞	far upstream

* Received 9 September 11998

*¹ Fluid Science Research Center

*² Advanced Technology Aircraft Project Center

*³ Aerodynamic Division

1. INTRODUCTION

Hybrid laminar flow control (HLFC), which combines suction laminar-flow-control (LFC) and natural-laminar-flow (NLF) concepts to achieve extensive laminar flow region over a wing surface is probably most applicable for wing chord Reynolds number to 40×10^6 and wing sweep angles between 20 to 30 degrees. The concept is of particular interest to near term transonic aircraft, because of being less complex than full chord LFC, requiring less suction and allowing the use of conventional wing box structure³). In 1990's several HLFC flight tests have been executed, for example, by using Boeing-757 HLFC wing test article¹⁰) and Airbus 320 HLFC engine nacelle¹¹) (see also a summary paper of reference 5) and transonic wind tunnel tests of HLFC swept-back wing have also been made^{6,12,13}). These studies have confirmed effects of suction HLFC, i.e. transition delaying and drag reduction effects. However, details of the suction systems such as a suction surface as well as suction duct systems have not been opened. Many design parameters are contained in the design

of HLFC wing and thus it is worthwhile to study various interesting combinations of the parameters. We have studied an improvement of the suction surface to find favorable geometric arrangement of great number of suction holes. It has been recognized that the hole itself becomes a roughness element and so too many holes would increase roughness effects and on the contrary too few holes would decrease the suction effect. Thus some favorable hole pattern would exist. An investigation of the pattern is a motive of the present study.

We had made an experimental study on HLFC with a two-dimensional airfoil in transonic and high Reynolds number flows⁷). Based on the experience, a three-dimensional swept-back HLFC wing model with a leading-edge partial-span suction system which contains a new suction hole arrangement (see section 2.1) was tested on its aerodynamic characteristics. The results of a transonic wind tunnel test are described in this report. We will observe that the wing can really produce not only fairly amount of drag reduction but also unexpected lift increase with very small amount of suction, the latter, as far as the present author knows, being the

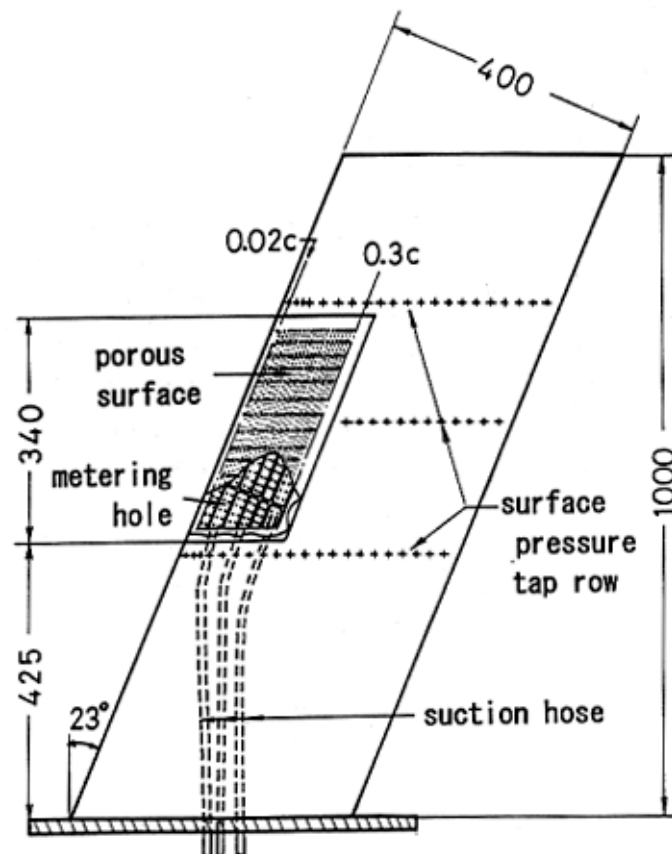


Figure 1 Geometrical outline of the wing model tested and the suction system

first observation in transonic HLFC/LFC investigations. We will also observe the effect of the suction on moment characteristics of the wing. These aerodynamic results confirms effectiveness of the suction surface used.

2. EXPERIMENT

2.1 Test model

An HLFC wing model used in the test is sketched in figure 1. It has a semi-span of 1m, a chord length normal to the leading edge of 0.40m which is constant in spanwise direction, and a swept-back angle of 23 degree. The airfoil section normal to the leading edge which is uniform in spanwise direction is so called 'NLAM78', a natural

laminar flow airfoil originally designed by the Boeing company⁴⁾ for a two-dimensional (2-D) one whose basic aerodynamic characteristics were reported in references 1 and 2. Design Mach number of the original 2-D airfoil is 0.77 so that, according to the simple sweep theory, corresponds to 0.84 in the present wing case. No three-dimensional optimum wing design has been made and thus the wing does not have any warp (camber and twist) and taper.

The partial-span leading edge suction system (see figure 1) is installed only on the wing upper surface with an expectation that it controls a cross-flow instability dominated in the leading edge surface region. Chordwise extent of the suction

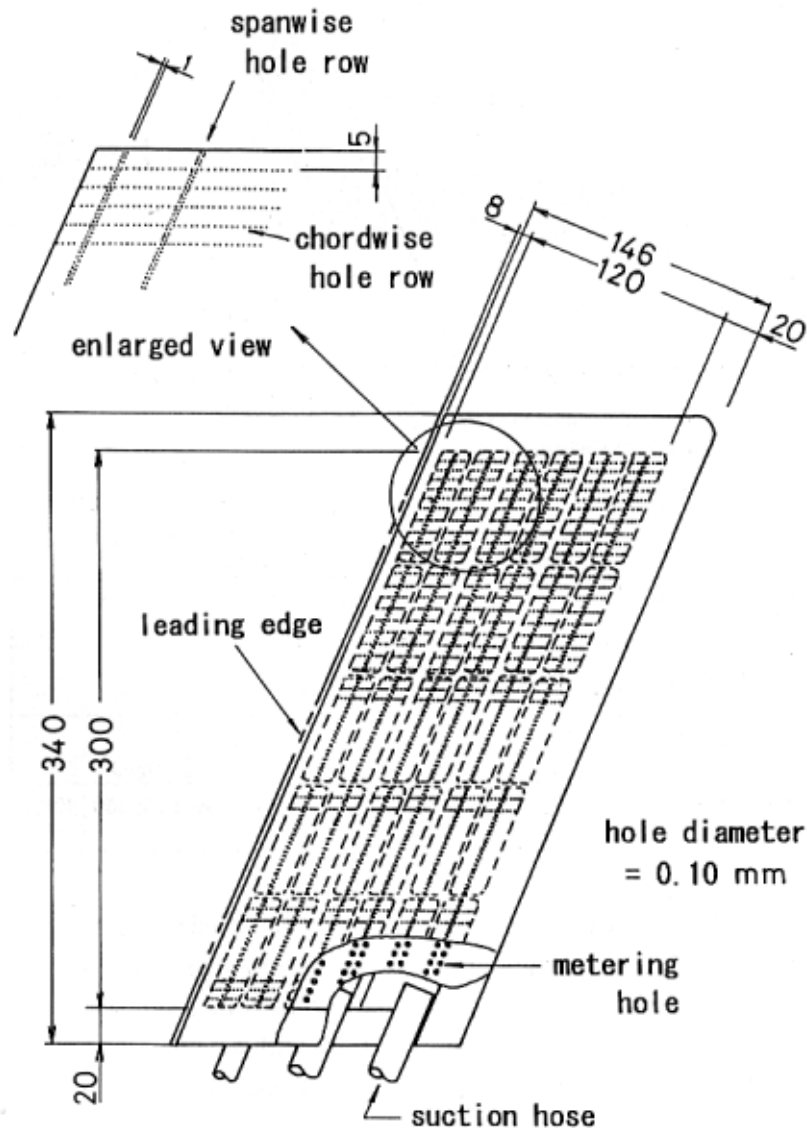


Figure 2 Details of the suction panel

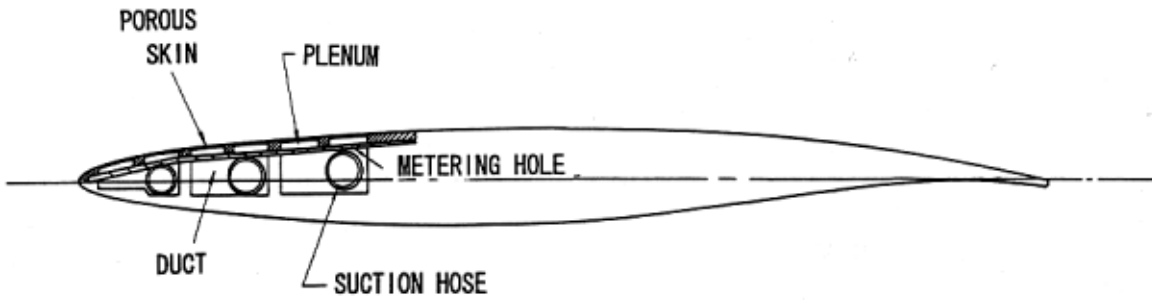


Figure 3 The suction system inside the wing model

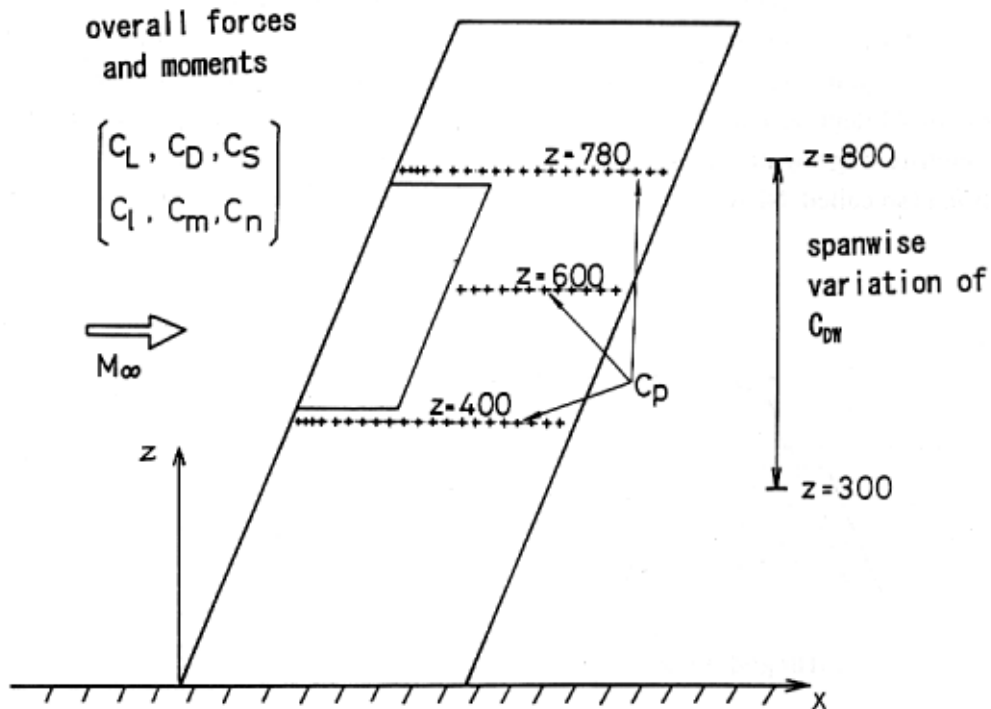


Figure 4 Position of static pressure tap rows and the spanwise range over which spanwise variation of wake drag is measured

Table 1 Test Conditions

Item	Symbol	Condition
Mach number	M_∞	0.54, 0.65, 0.76, 0.82, 0.84, 0.86, 0.88, 0.90, 0.92
Angle of attack	α	$-1^\circ, 0^\circ, +1^\circ$
Suction quantity	Q_T (litre/min.)	0~40, uniform and/or distributed suction
Wake traverse	z (mm)	300, 350, 400, 450, 500, 550, 600, 650, 700, 750, 800

region (about up to 20% chord line) was determined from a consideration that we will use the wing box structure ahead of a front spar of a real wing which is usually placed at nearly 20% chord. The system uses a suction skin with many holes specially arranged not to produce significant disturbance (figure 2) and a suction duct system (figure 3) which

has been tested successfully^{7),9)}. The idea of the hole arrangement is to decrease total number of holes by combining a slot suction concept (spanwise hole row) with a perforated suction one (chordwise hole rows). Suction flow quantity in each collect duct can be adjusted separately. The reason why the partial-span leading-edge suction system is adopted



Figure 5 Wing model and Pitot rake setup in the wind tunnel test section

is mainly due to severe structural constraints, which as will be shown later prevents us from getting significant drag reduction rate by suction expected from large reduction rate of the wake drag.

Surface static pressure tap rows are located at spanwise positions of $z = 400, 600$ and 780mm (figure 4). Note that the pressure is measured only on a non-suction surface region at $z = 600\text{mm}$.

2.2 Measurements and Test conditions

Tests were conducted in the transonic wind tunnel of National Aerospace Laboratory, whose test section has a dimension of $2\text{m} \times 2\text{m}$ (figure 5). We measure overall forces (lift, drag and side force) and moments (pitching, yawing and rolling) by using a six-components external balance, and the surface pressure distributions with and without suction. Also a static and a total pressures in a wake flow were measured to evaluate a section profile drag at several spanwise positions between $z = 300\text{mm}$ and 800mm (figures 4 and 5). The test conditions are summarized in table 1.

3. RESULTS AND DISCUSSION

3.1 Surface pressure distribution

Surface pressure distributions at $M_\infty=0.84$ (the design Mach number) when suction is not applied are shown in figure 6. Favorable pressure gradient, characteristic to the natural laminar flow airfoil, is well observed except wing tip region ($z = 780\text{mm}$) where the gradient is maintained only up to 40% chord point for all angles of attack. The lost of the favorable pressure gradient and spanwise similarity of the C_p distribution is mainly attributed to the lack of any proper three-dimensional design of the basic wing. As the Mach number decreases from the design point, the spanwise similarity is fairly recovered, but the favorable pressure gradient becomes smaller, as is shown in figure 7.

Figure 8 shows surface pressure distributions when suction is applied. Compared with the non-suction case (figure 6), the suction produces only a little increase of suction pressure in the rearward region. However the overall effect of suction on the pressure distribution is not clear, because no lower surface pressure was not measured.

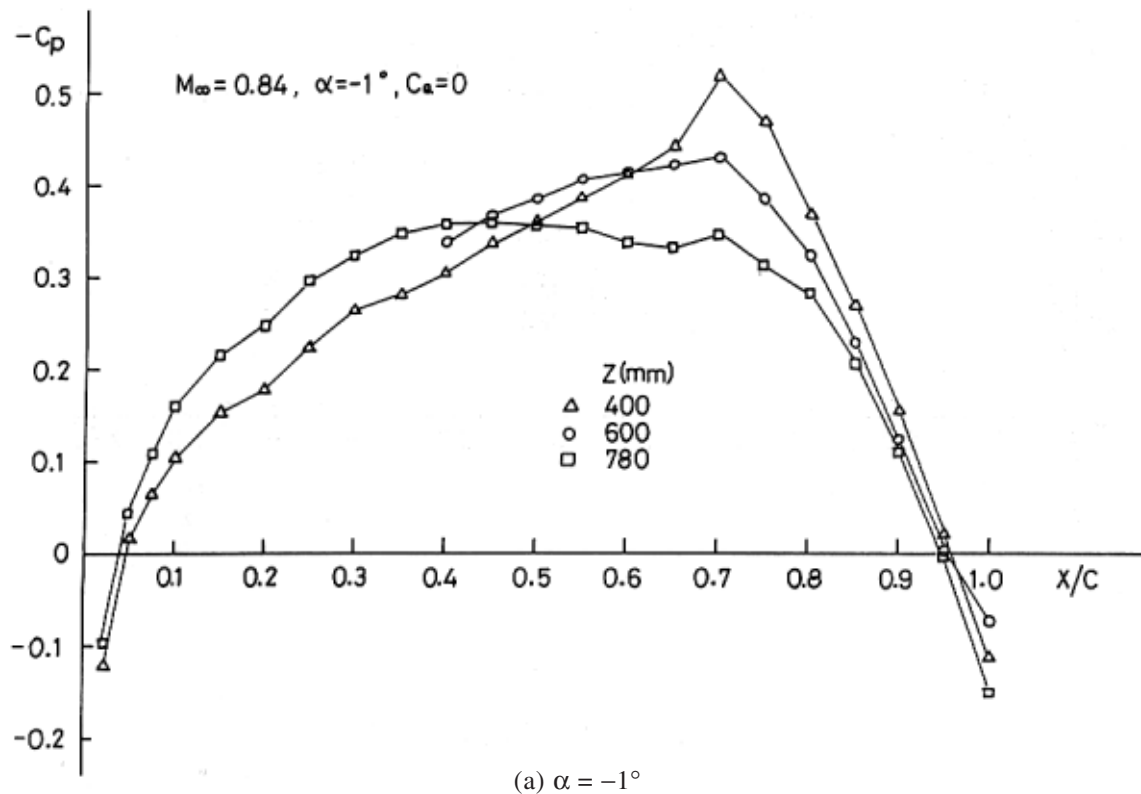


Figure 6 Measured surface pressure distributions at the design Mach number $M_\infty = 0.84$ (without suction)

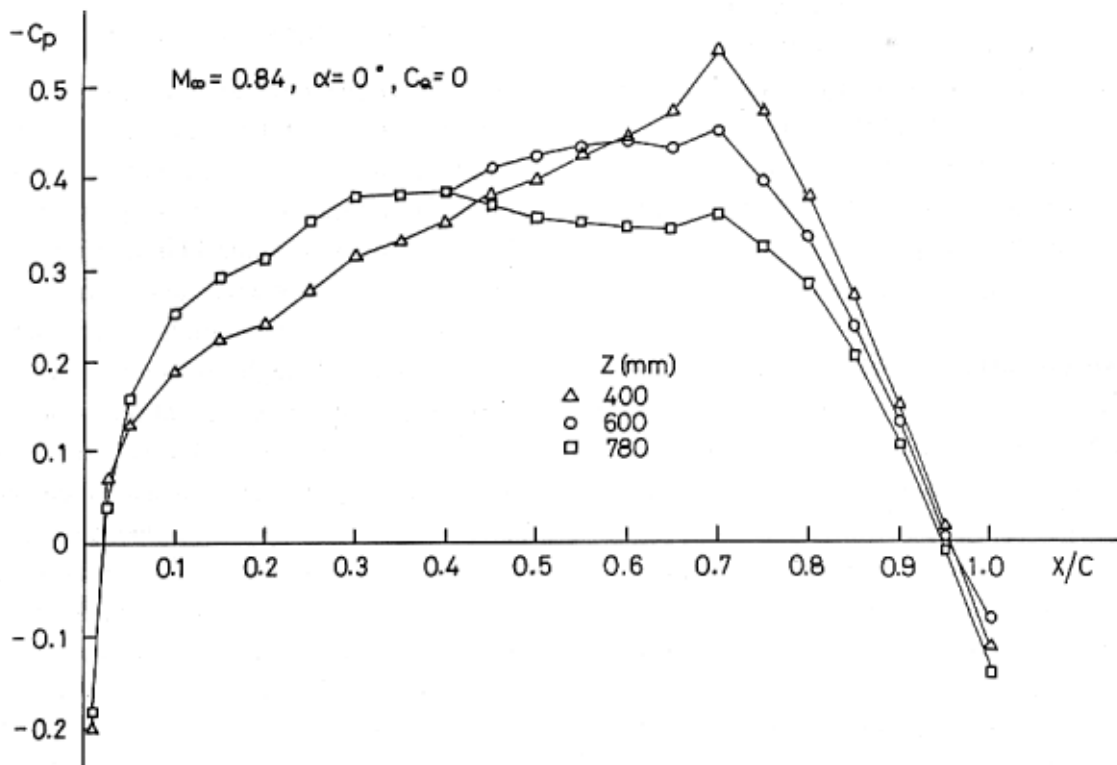
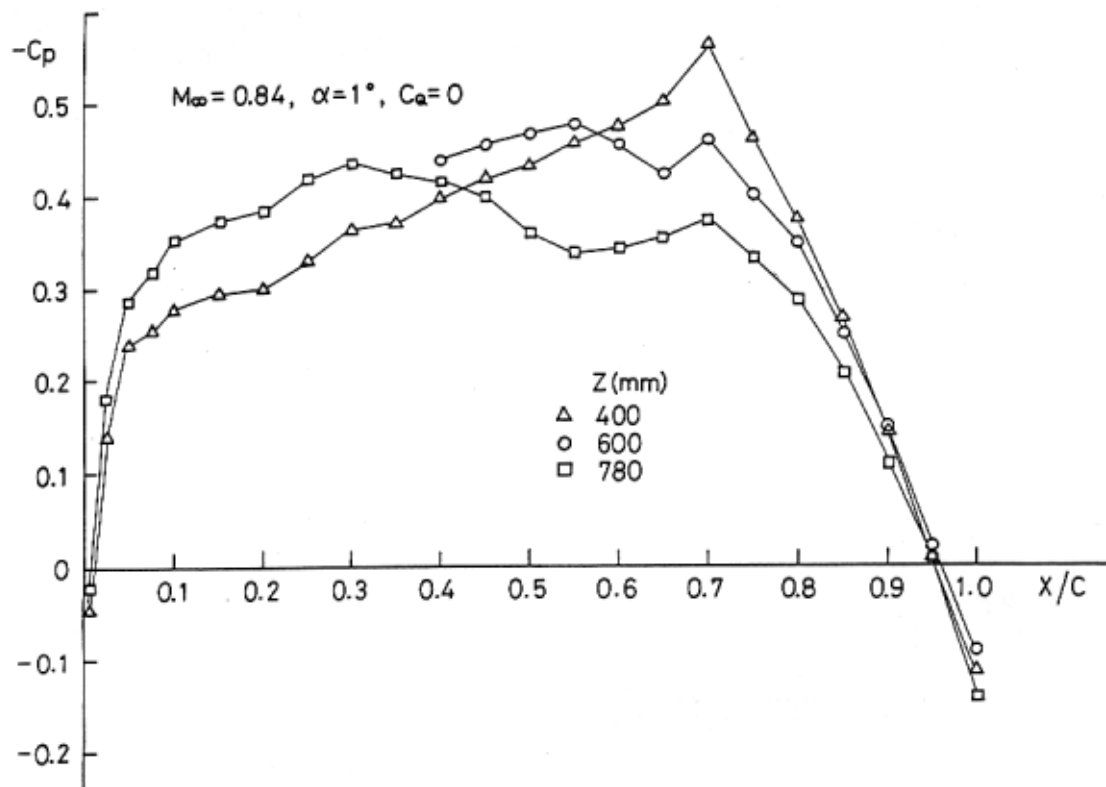
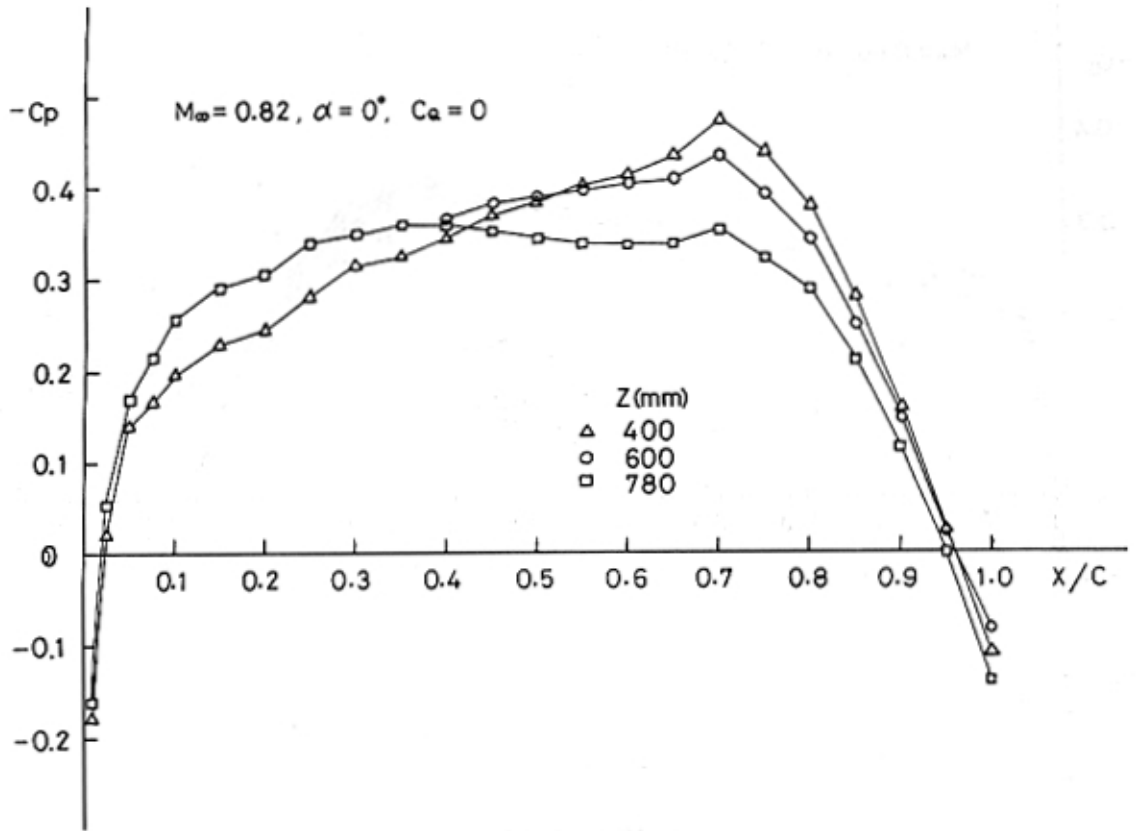
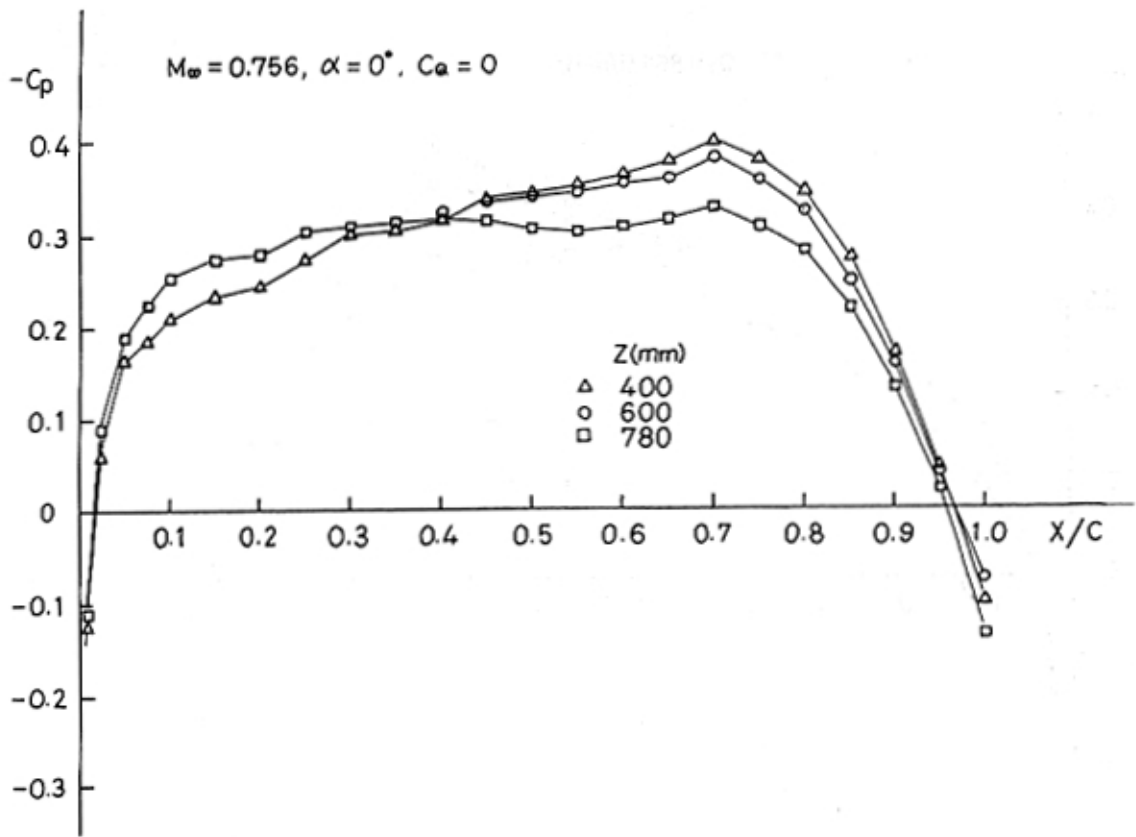
(b) $\alpha = 0^\circ$ (c) $\alpha = 1^\circ$

Figure 6 (Continued)

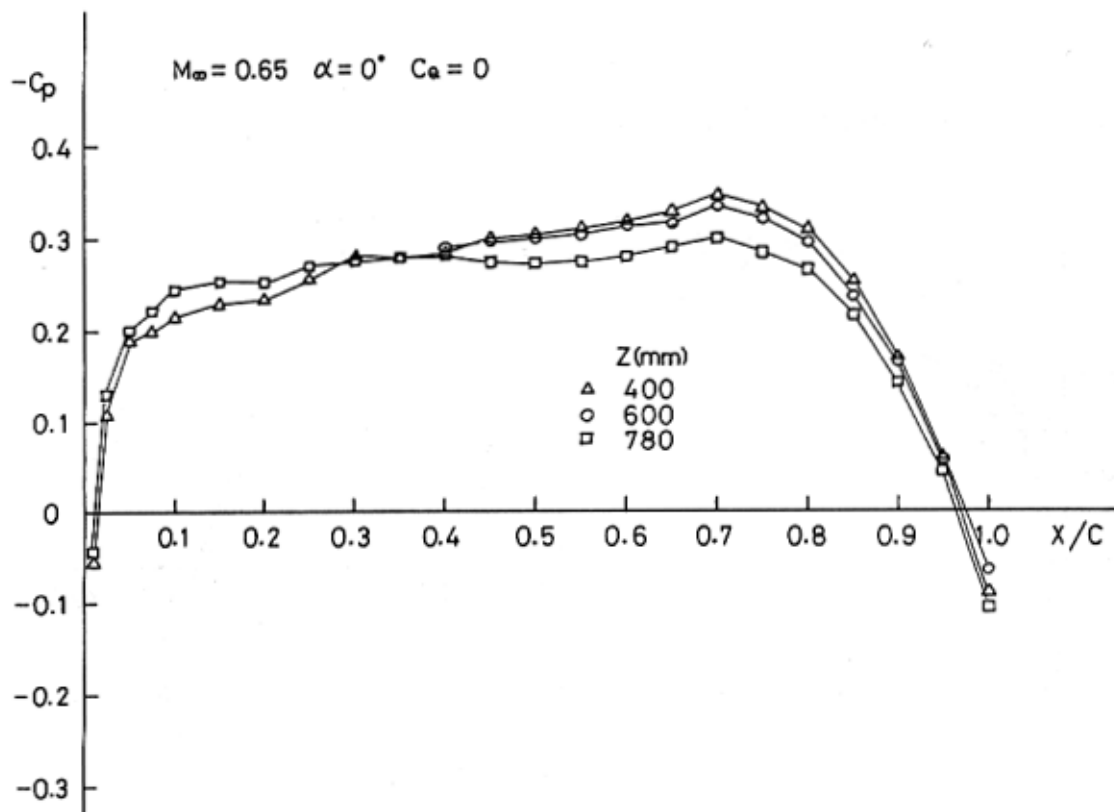


(a) $M_\infty = 0.82, \alpha = 0^\circ$



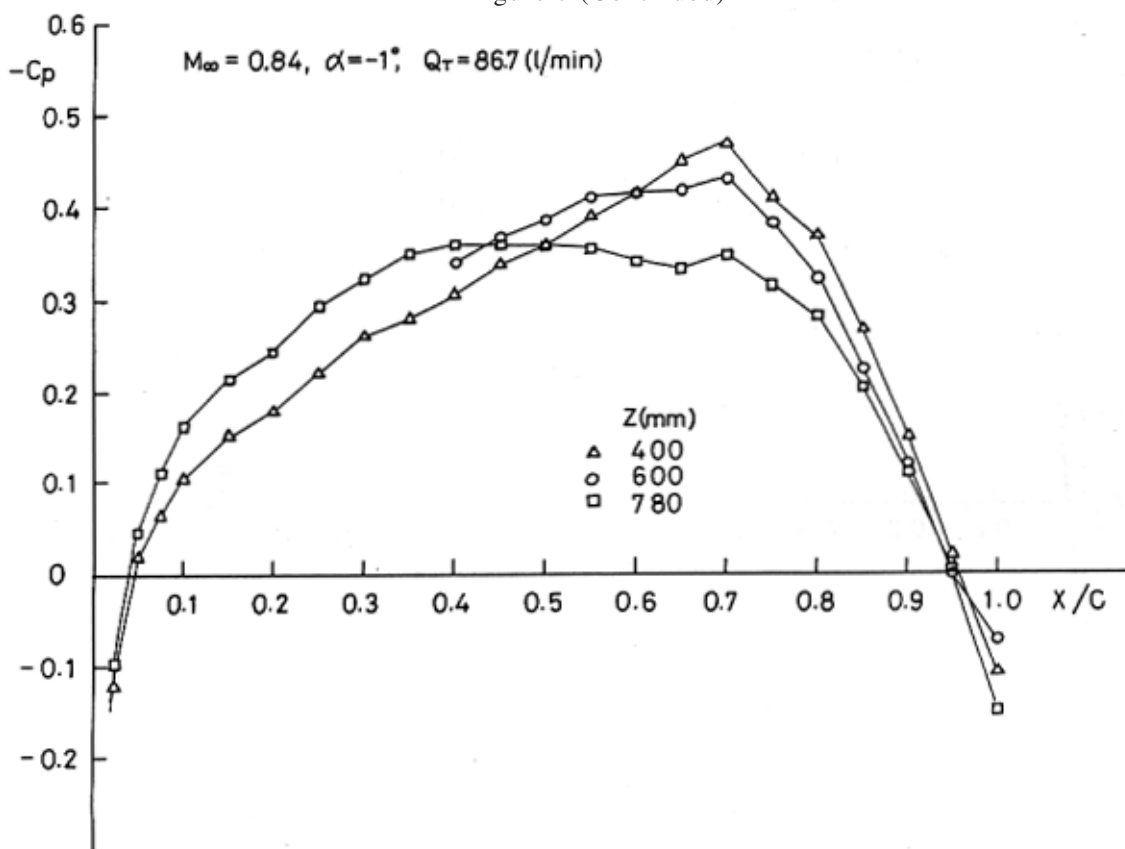
(b) $M_\infty = 0.756, \alpha = 0^\circ$

Figure 7 Measured surface pressure distributions at the off-design Mach numbers (without suction)



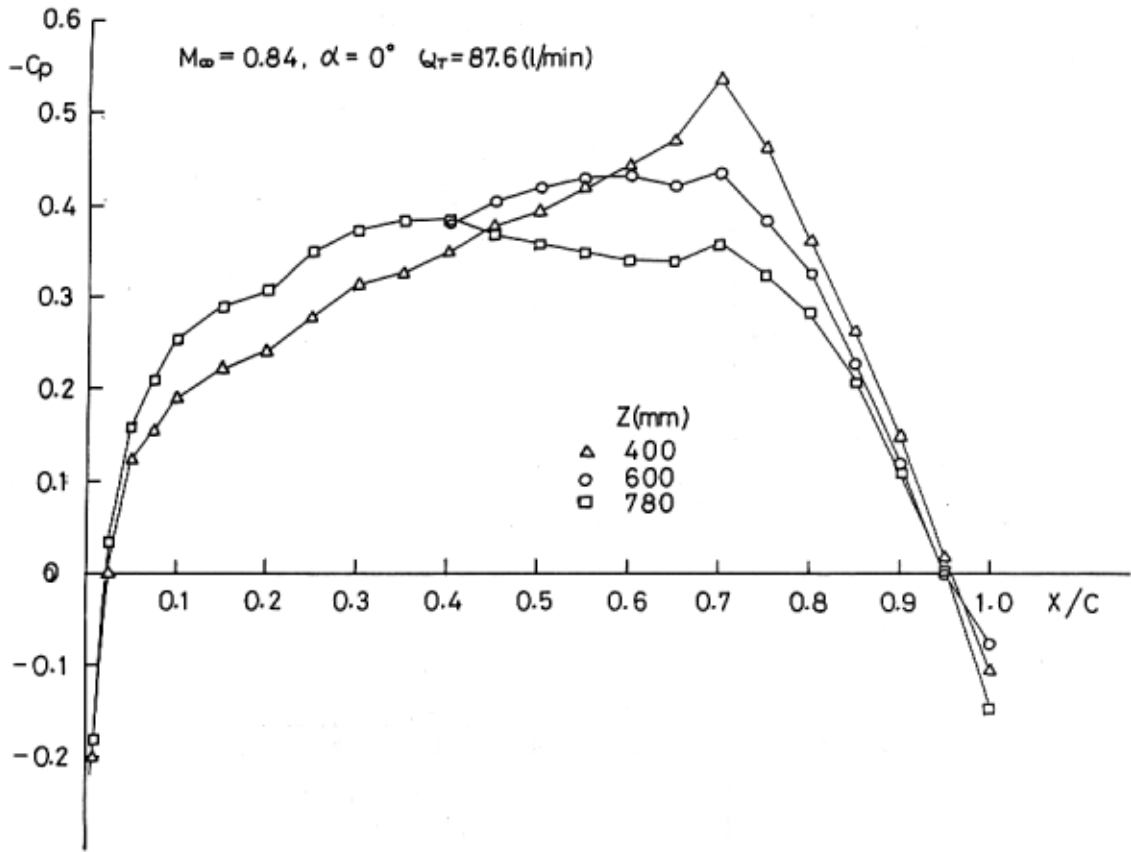
(c) $M_\infty = 0.65, \alpha = 1^\circ$

Figure 7 (Continued)

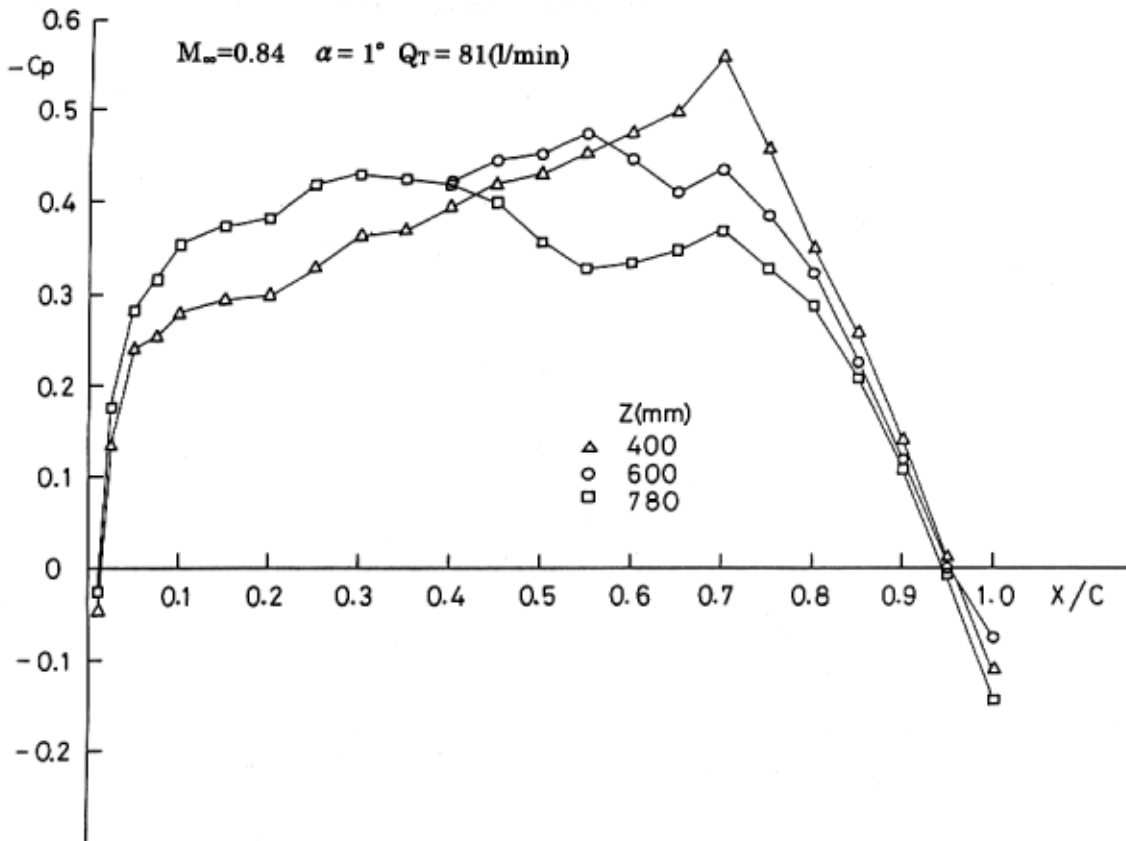


(a) $\alpha = -1^\circ, Q_T = 86.7 \text{ (l/min)}$

Figure 8 Measured surface pressure distributions at the design Mach number $M_\infty = 0.84$ (with suction)

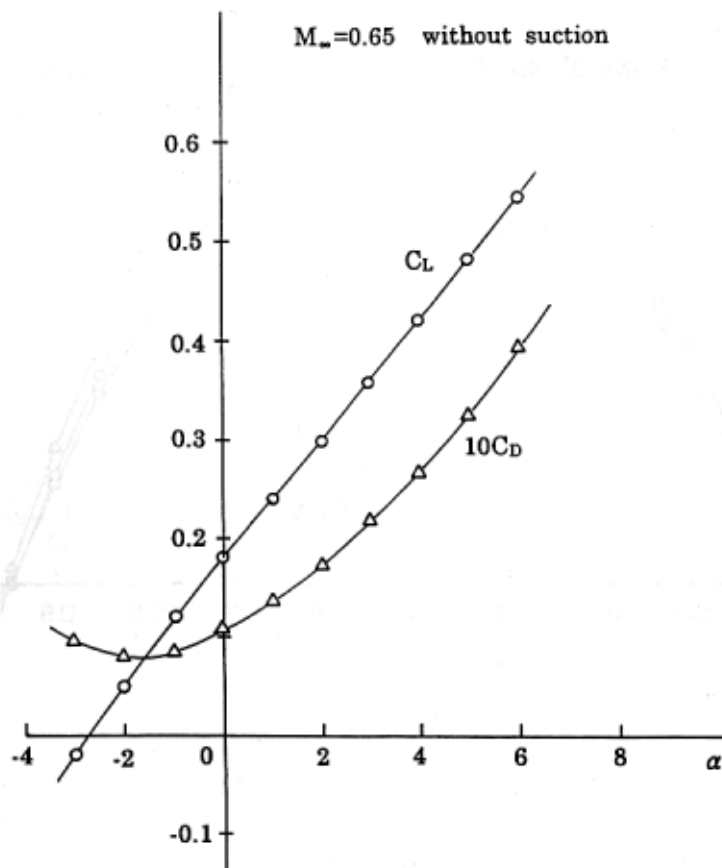


(b) $\alpha=0^\circ, Q_T=87.6 \text{ (l/min)}$

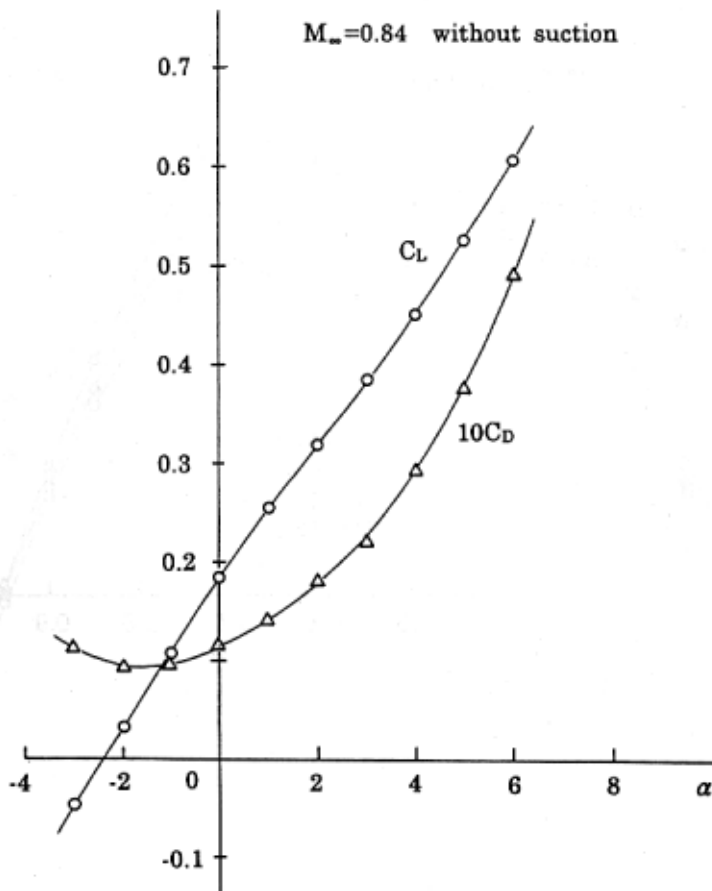


(c) $\alpha=1^\circ, Q_T=81 \text{ (l/min)}$

Figure 8 (Continued)



(a) $M_\infty=0.65$



(b) $M_\infty=0.84$

Figure 9 C_L and C_D plotted against angles of attack (without suction)

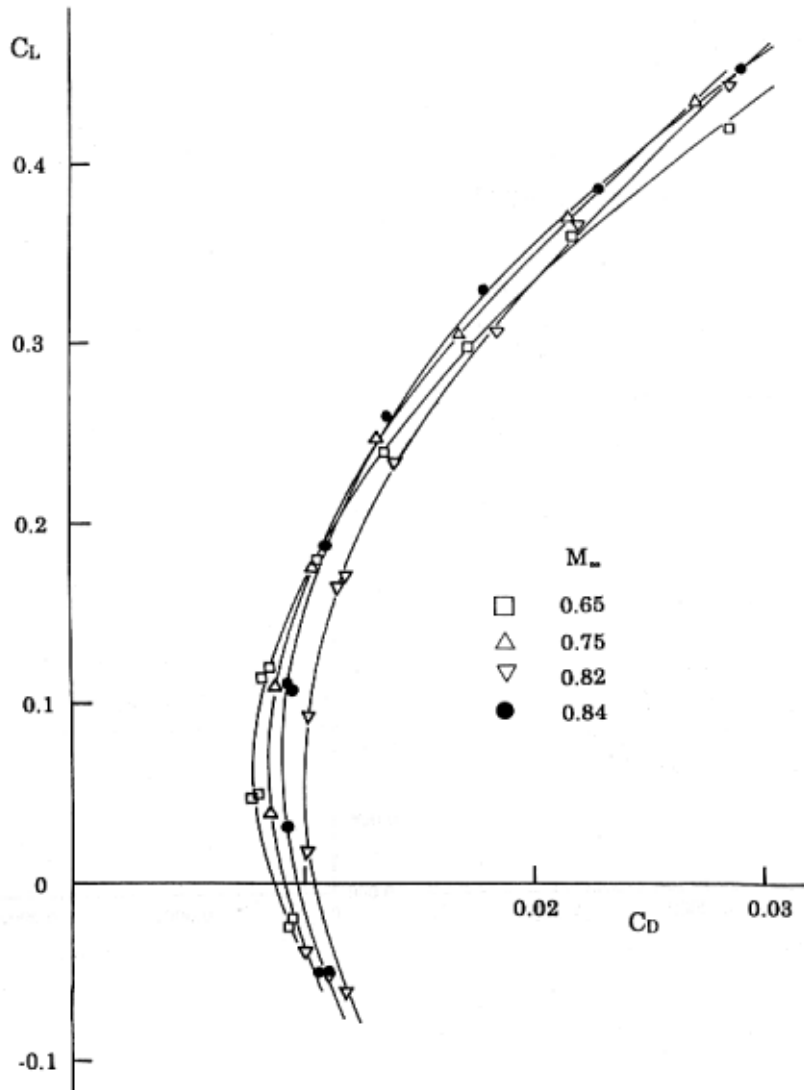


Figure 10 Drag polar curves (without suction)

3.2 Forces and moments

3.2.1 Overall force and moment characteristics of the wing

Overall lift and drag coefficients of the wing without suction are plotted against angle of attack α at $M_\infty = 0.65$ and 0.84 in figures 9(a) and (b), respectively. A lift curve slope at $M_\infty = 0.84$ is larger than that at 0.65 and the drag is slightly higher at $M_\infty = 0.84$ than 0.65 . Figure 10 shows drag polar curves when the suction is not applied. At lower C_L the drag coefficient takes smaller value for the lower Mach numbers and at higher C_L , vice versa. No systematic drag polar curve measurements were made when suction is applied.

In figure 11, the overall drag coefficient C_{DB} is plotted against a total suction flow quantity coefficient, defined by

$$C_Q = \int_0^1 \frac{\rho_w v_w}{\rho_\infty U_\infty} d(x/c), \quad (1)$$

for various Mach number and angles of attack α . The drag reduction by suction can be observed except a few cases, although the effect is not significant. For example, at $M_\infty = 0.84$ the maximum drag reduction rate is only 1.7 and 2.1% at $\alpha = 0^\circ$ and -1° , respectively and no suction effect is observed at $\alpha = +1^\circ$. The reason why the drag reduction rate remains smaller than expected is, as was already stated, mainly due to the shortage of the spanwise extension of the suction area. As will be shown later, the suction certainly produces large reduction of a section wake drag C_{DW} in a plane just downstream of the suction surface region and so if a full span suction system were employed,

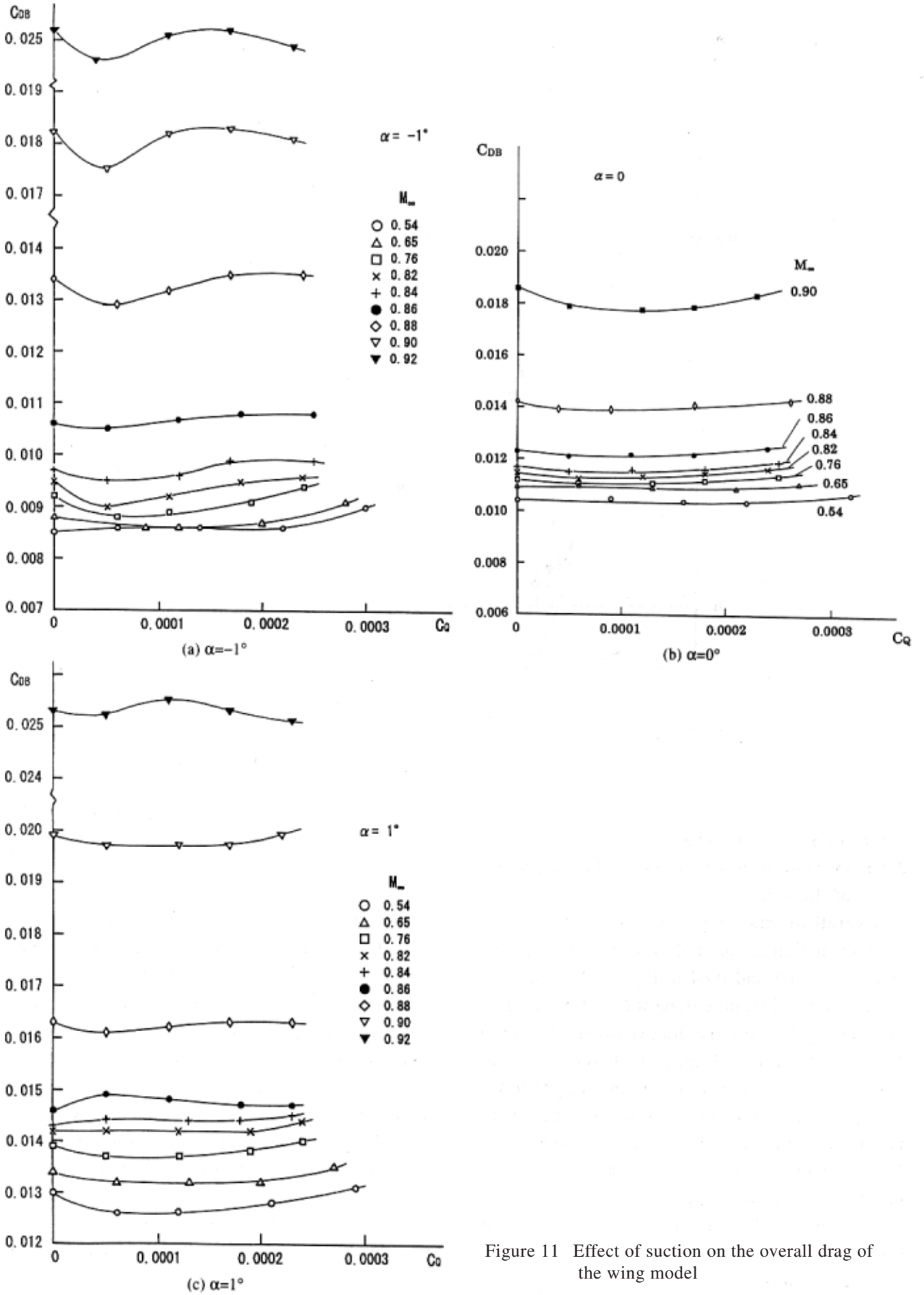


Figure 11 Effect of suction on the overall drag of the wing model

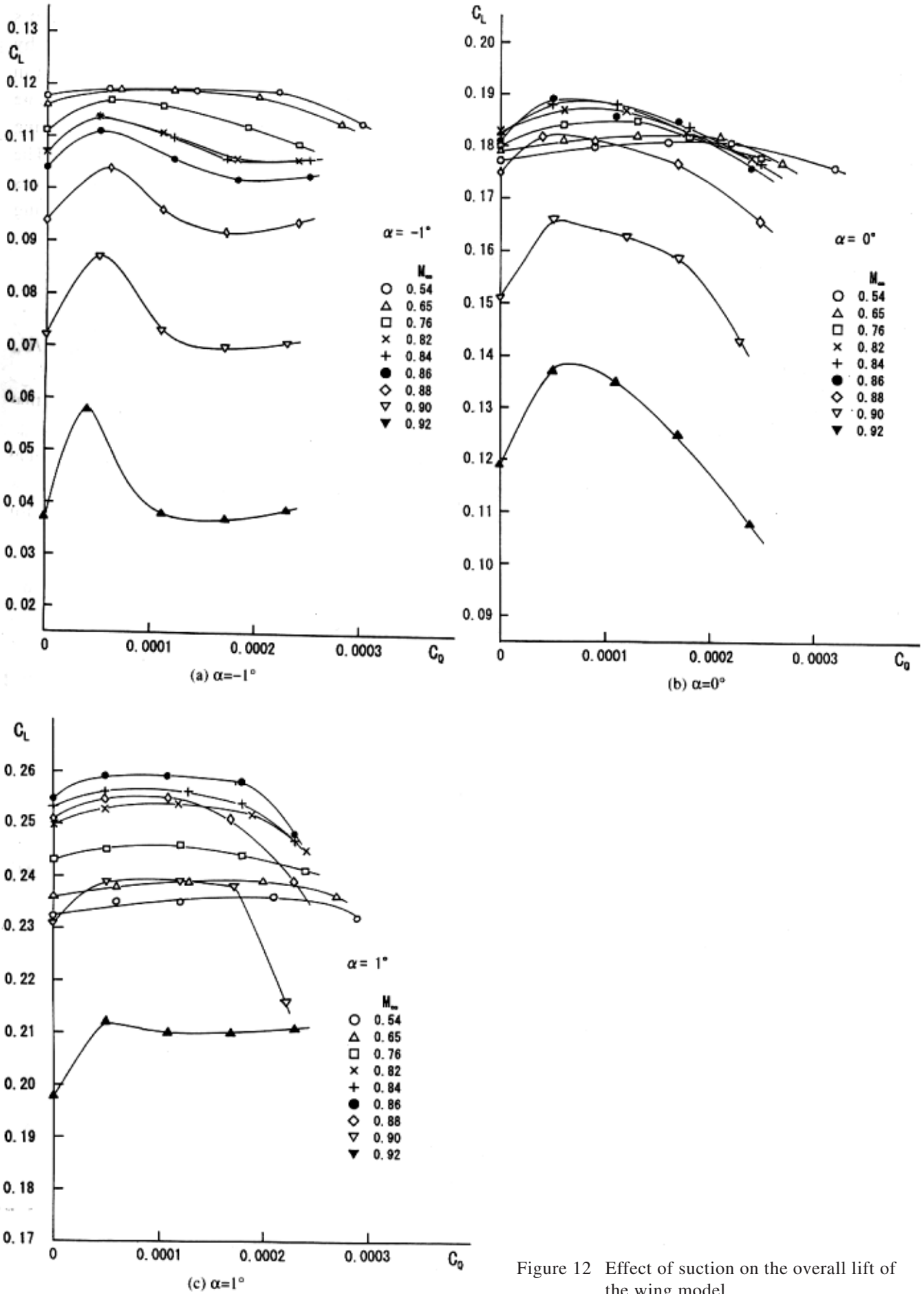


Figure 12 Effect of suction on the overall lift of the wing model

larger drag reduction rate could be expected in total.

Figure 11 shows that an optimum suction flow quantity C_{QDmin} exist, at which the drag coefficient becomes minimum for each flow condition and that the drag reduction rate is significant for Mach numbers higher than 0.9 at which the drag value itself is high. The latter suggests that the suction could improve drag characteristics of an aircraft in high transonic Mach number region.

Figure 12 shows an effect of suction on a lift coefficient C_L . It is observed for Mach numbers greater than 0.76 that as the suction increases from zero, the lift coefficient first increases to the maximum value and then decreases. The maximum rate of increase is , for example, 3% at $M_\infty = 0.84$ and $\alpha = 0^\circ$. It is also observed for each Mach number and angle of attack that an optimum suction flow quantity C_{QLmax} exists at which C_L becomes maximum. It is very interesting to note that the

C_{QLmax} is very near the C_{QDmin} . To the author's knowledge, the increase of lift coefficient by boundary layer suction is the first observation in transonic flows. (The first author observed same lift increase phenomenon in a low speed LFC wing test⁹⁾.) What is the reason of the lift increment? The control surface momentum theorem for the forces acted on a wing gives the lift coefficient of the wing as

$$C_L = C_{L0} + 2 \int \frac{\rho_w}{\rho_\infty} \left(\frac{v_w}{U_\infty} \right)^2 d \left(\frac{S_\perp}{S_w} \right) \quad (2)$$

where C_{L0} represents the part which does not include suction velocity term explicitly. As the term v_w/U_∞ is 0 (10^{-3}) in the present test, the second term of the right hand side is negligible compared to C_{L0} , that is to say, the direct suction effect on the lift coefficient is negligible. Therefore the lift increment by suction is mainly due to secondary induced flow changes. The flow changes can be seen from, for

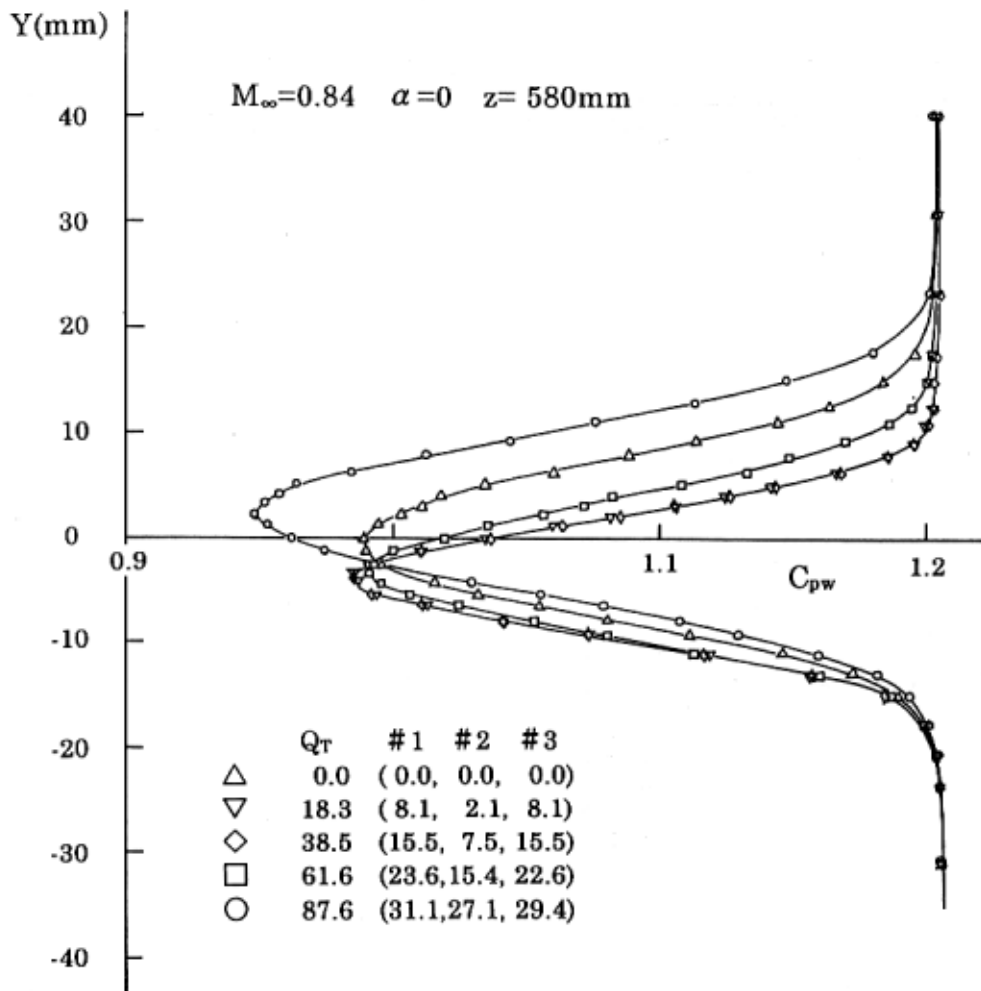


Figure 13 Effect of suction on the shift of the wake center at $M_\infty = 0.84$, and $\alpha = 0^\circ$ (Upward shift in the figure means in reality downward shift of the wake.)

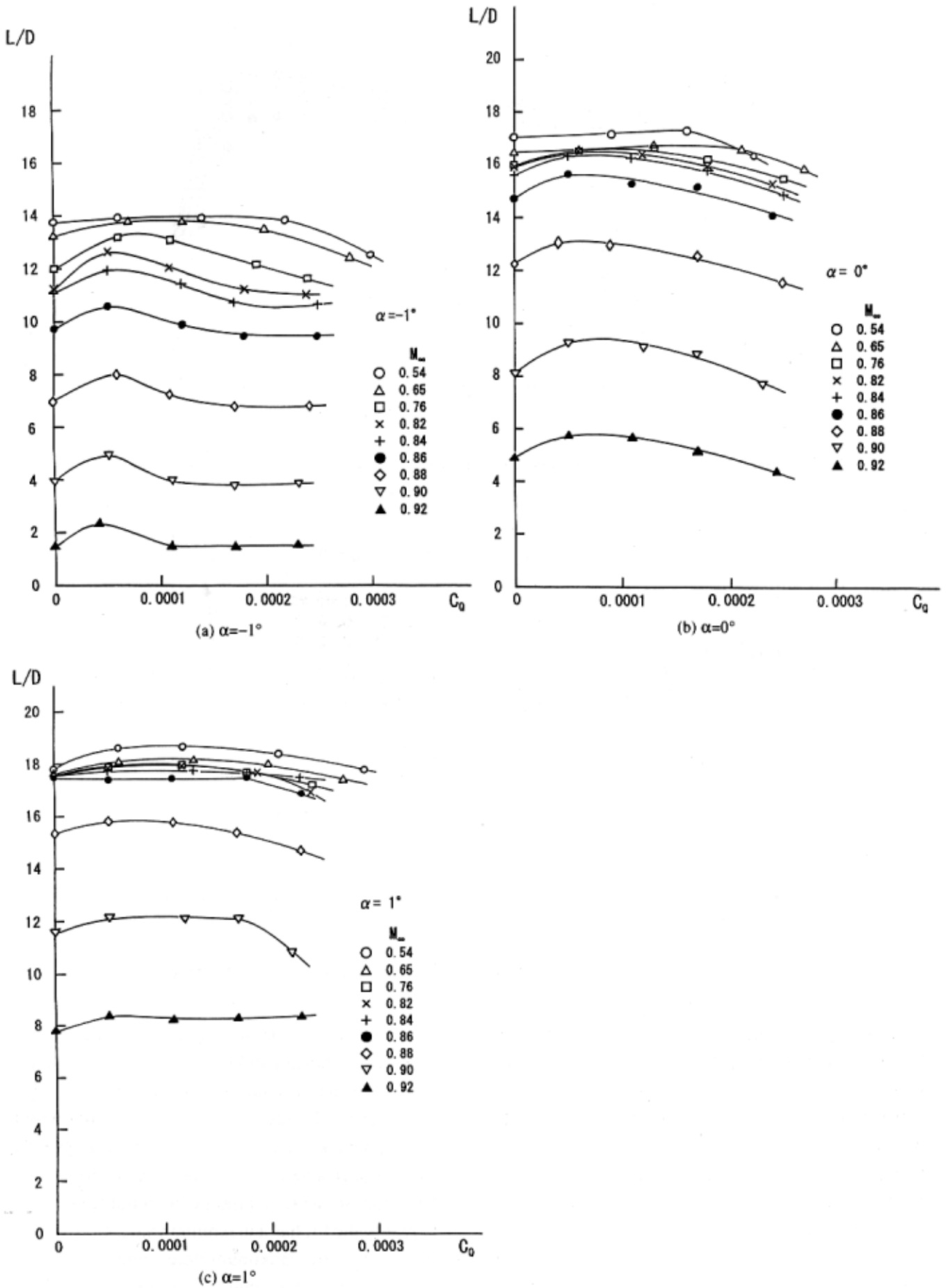


Figure 14 Effect of suction on the Lift to drag ratio, L/D

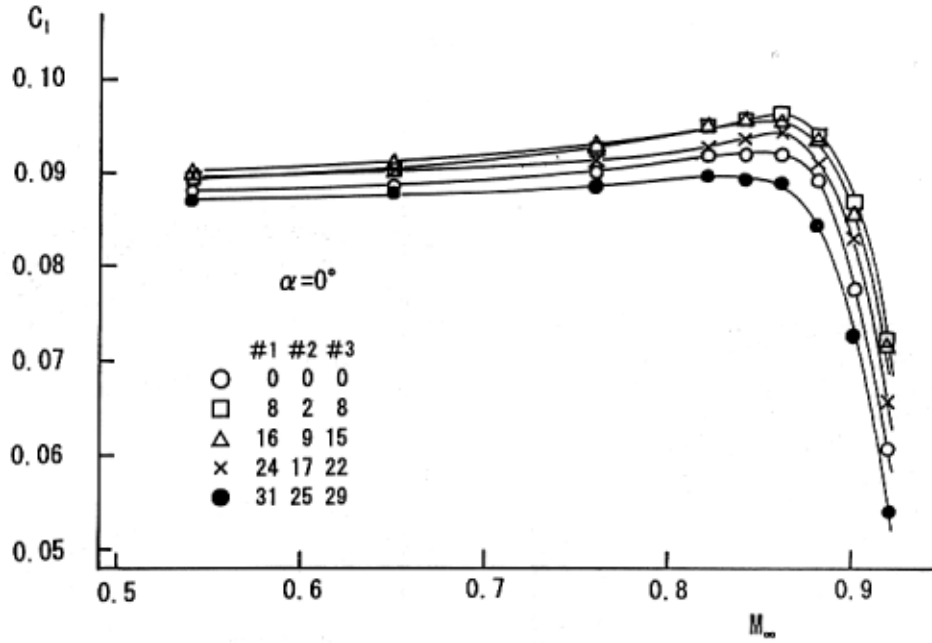


Figure 15 Mach number variation of the effect of suction on the rolling moment of the wing model

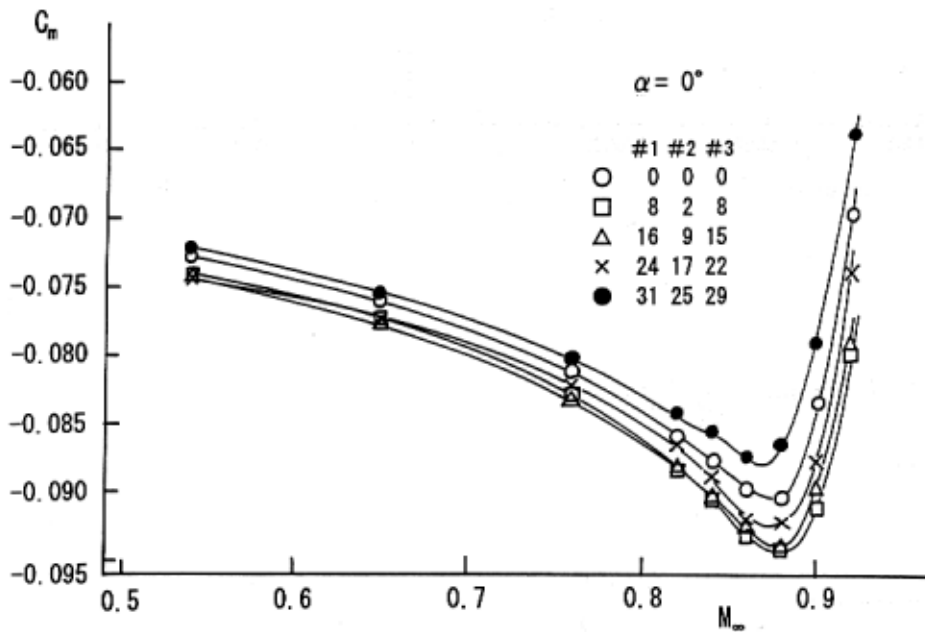


Figure 16 Mach number variation of the effect of suction on the pitching moment of the wing model

example, vertical movements of the wake profiles. Figure 13 shows a total pressure profiles measured in the wake flow and we can see that the wake center shifts downward to the wing lower side (upper side of the figure) as the suction quantity increases, which suggests downward turning of the wake flow i.e. the lift increase of the wing. (Direct and crucial evidence may be obtained from the both upper and lower surface pressure data, but in the present case only the upper surface one is available.) However,

the physical reason why the lift maximization occurs is not always straight-forward. We first come to an idea that a reduction of the boundary layer thickness by the suction recovers a lift loss which is caused by the viscous effect. But if it always were true, the lift would have to increase continuously with suction to an asymptotic potential flow value: in reality the lift has a maximum value. Considering the fact that the maximum drag reduction and lift increment occurs at almost the same C_Q (i.e. $C_{Q_{Lmax}}$

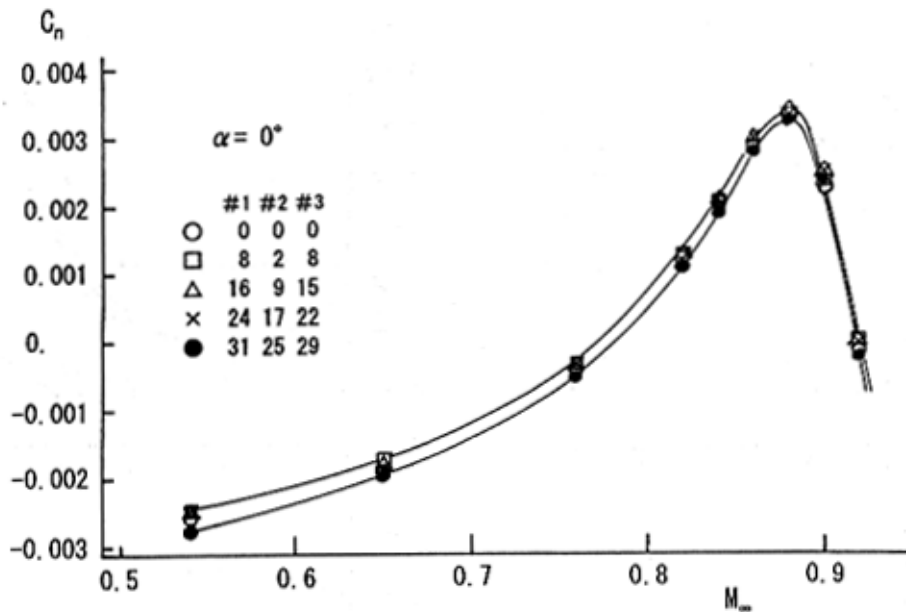


Figure 17 Mach number variation of the effect of suction on the yawing moment of the wing model

$\sim C_{QDmin}$) it may tentatively be said that a transition position or equivalently an extent of a thin (laminar) boundary layer over the wing is nearly critical at the suction quantity C_{QLmax} and a larger C_Q would cause a premature transition which extends a thicker (turbulent) boundary layer region which in turn results in the lift loss and drag increase.

The lift increasing effect of suction can produce a larger lift to drag ratio L/D than expected from the drag reduction alone. For example, the maximum increment rate attains to about 4.5% at Mach number of 0.84 and $\alpha = 0^\circ$ as is shown in figure 14(b). If the suction would produce only drag reduction, the corresponding value would become 1.7%. The rate amounts to 7.2% at $\alpha = -1^\circ$, but it is not so large at $\alpha = +1^\circ$. The lift increasing effect is quite favorable to the application of HLFC technology in transonic flows and a further study will be required to get deeper understanding of a true mechanism of the lift increment.

We now turn our attention to moment coefficients. Figure 15 shows the rolling moment coefficient C_l plotted against Mach number at $\alpha = 0^\circ$. In this and following two figures symbols #1, #2, and #3 means the first, second and third collect duct, respectively and the numerical values under these symbols represent the suction flow quantity in *litre/min*. Application of a moderate suction makes the moment increase, but an excessive one

(●) decrease. The moment depends much on the suction as the lift force which governs the moment does. The same is true for the pitching moment C_m shown in figure 16 whose variation with suction is similar to that of the rolling moment. The yawing moment, on the contrary, depends little on the suction (figure 17), because it is closely related to the drag force which also depends little on the suction. As a summary, it is concluded that the moments associated with out-of plane force (lift) are very sensitive to the suction and the ones associated with in-plane forces (drag and side force) are not. The sensitivity of the moments with surface suction seems to suggest a possibility of moment control by suction in transonic flow.

3.2.2 Section wake drag

Now we turn our attention to the section wake drag C_{DW} which is obtained from two-dimensional wake flow quantities measured at several spanwise (z) positions. We have used the wake drag formula given by Holder et al.¹⁴⁾ Figure 18 shows the drag coefficient measured at $z = 580\text{mm}$, a plane just downstream of the suction surface region, for some Mach numbers and angles of attack α . The equivalent suction drag⁸⁾ which equals to a nondimensional value of a suction power in terms of the drag coefficient is also included in the wake drag. Significant drag reduction is established at $\alpha = 0^\circ$,

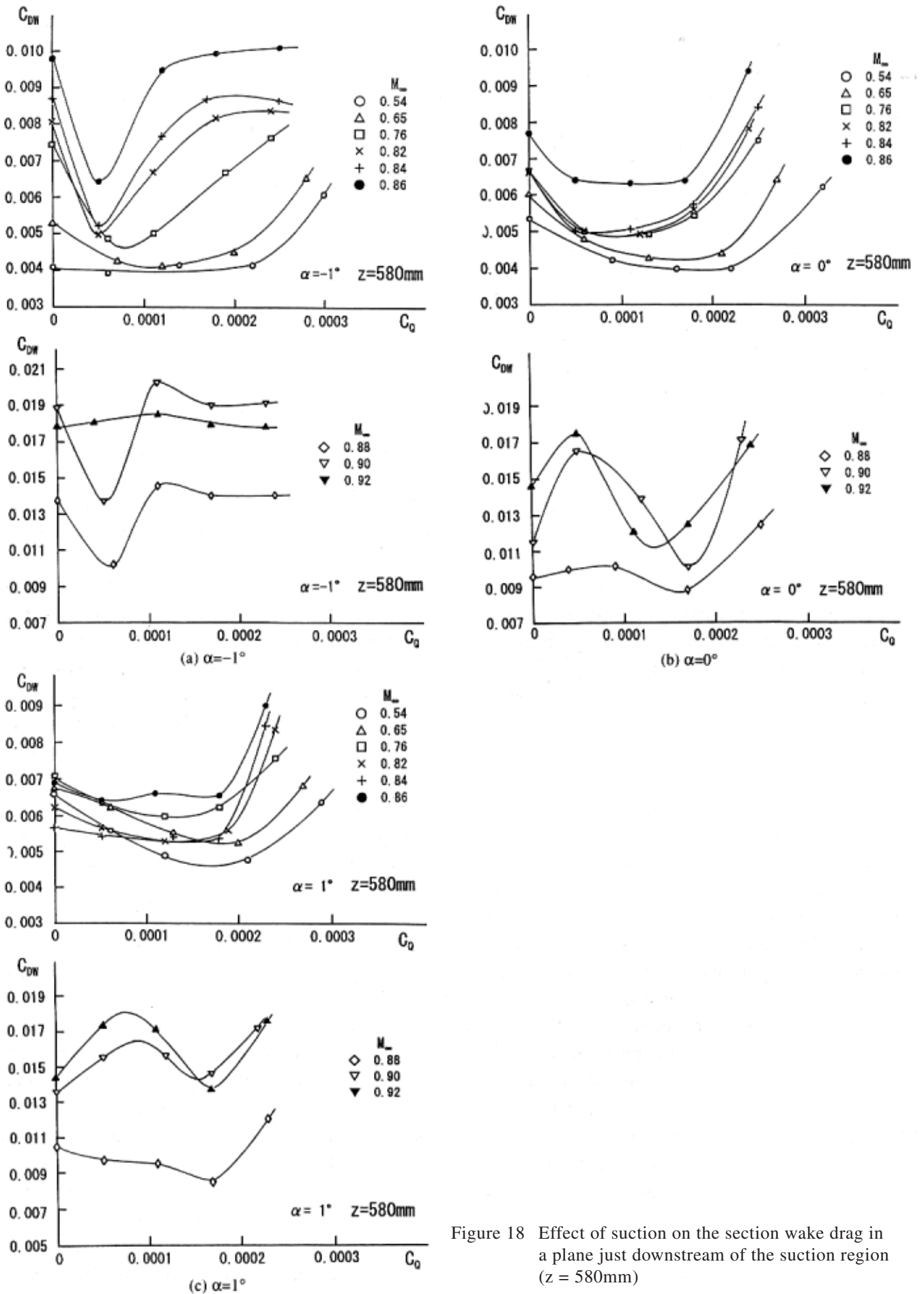


Figure 18 Effect of suction on the section wake drag in a plane just downstream of the suction region ($z = 580\text{mm}$)

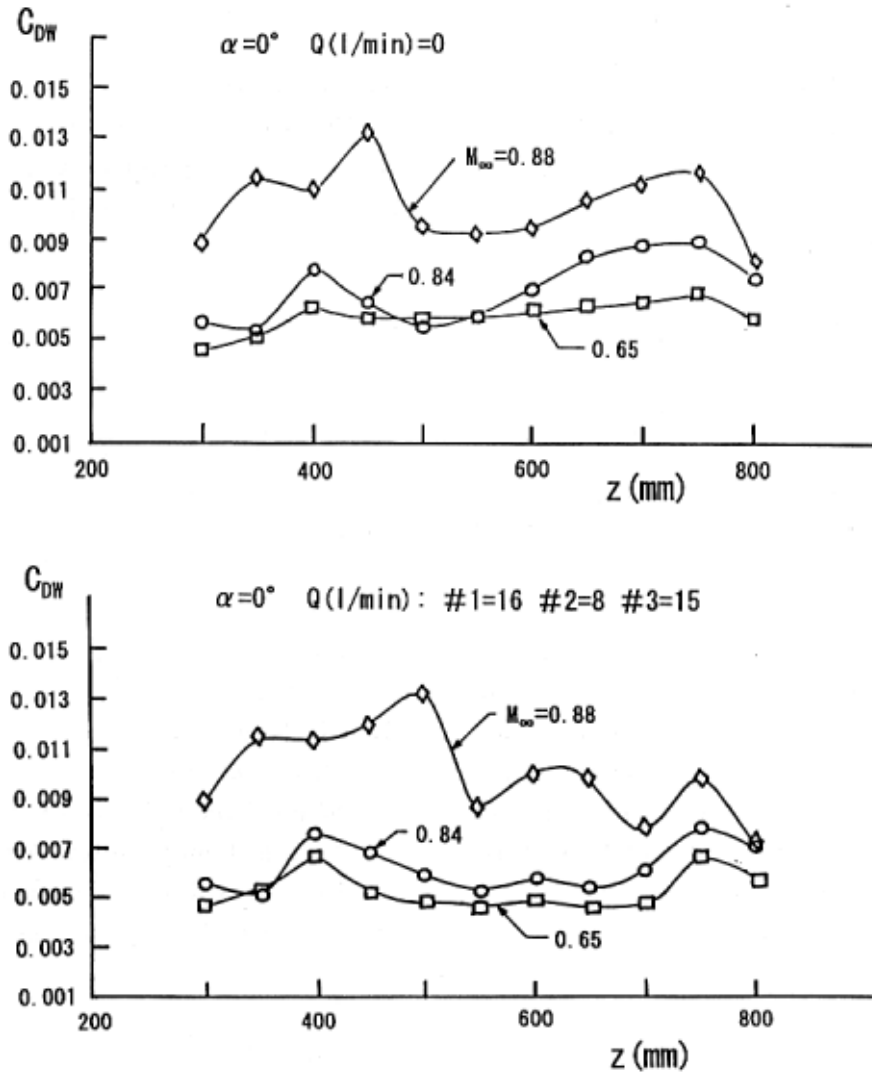


Figure 19 Spanwise variation of the section wake drag with and without suction

and the maximum drag reduction rate is beyond 20% for a wide range of C_Q when Mach number is less than 0.88. Fairly large drag reduction is also observed at $\alpha = -1^\circ$ for $0.76 \leq M_\infty \leq 0.86$ with narrower effective C_Q range. However, at $\alpha = +1^\circ$, the suction effect becomes considerably small. It is known that some estimation error is inevitable in the evaluation of the wake drag by the wake traverse method associated with small nonzero values at wake edges in transonic flows. However the drag reduction rates stated above are all far beyond the estimated error band and so the conclusion above stated remains unchanged even when the error is taken into account. It is also noted that we repeated the test twice and confirmed reproduction of the data within the error band.

We have discussed above the suction effect in the section just downstream of the suction region.

Now we will investigate spanwise variations of the section drag. Figure 19 shows the typical variations of C_{DW} with and without suction for $M_\infty = 0.65, 0.84$ and 0.88 . Note that the suction surface occupies a region from $z = 450\text{mm}$ to 750mm . It can be seen at $M_\infty = 0.65$ and 0.84 that C_{DW} certainly decreases over downstream of the suction region when the suction quantity written in the figure is applied and also the spanwise variations becomes small. However at $M_\infty = 0.88$ the suction effect is no longer observed and the spanwise variation is rather large. At this Mach number local shock waves appear on the wing surface which prevent the achievement of the drag reduction and spanwise smooth variation. It is observed that the section drag is higher at $z = 400\text{mm}$ than other positions at $M_\infty = 0.65$ and 0.84 . It is due to a premature boundary layer transition caused by the surface pressure tap row placed in

this plane.

3.2.3 Background disturbance

The present HLFC test has been executed in a wind tunnel test section with perforated walls and so its background disturbance level is a little too high. Nevertheless the drag reducing effect of the HLFC wing in terms of the section wake drag is clearly confirmed over a wide range of transonic Mach number. The Reynolds number based on the chord length normal to the leading edge is about 7.7×10^6 at $M_\infty = 0.84$. Even at Mach numbers higher than M_{DD} the drag divergent Mach number, at which strong local shock waves are generated on the wing surface, the leading edge suction seems to still work well, the drag reduction rate sometimes being larger than that at Mach numbers less than M_{DD} . This means that the leading edge suction system has good off-design performance. It is very interesting to ask again why the leading edge suction works well even at Mach numbers higher than M_{DD} . To answer it, more detailed flow measurement should be made in the flow region.

5. SUMMARY

We have made a transonic wind tunnel test of an HLFC wing model with a new leading edge suction system incorporated with a natural laminar flow airfoil to check drag reducing effect of the suction system in transonic Mach number range. The suction system has produced significant reduction of the section wake drag by very small amount of suction, although the reduction rate of the overall drag remains modest due to the limited suction surface area. The suction system is also effective at off-design Mach numbers. Besides the drag performance, we have made an interesting observation for a wide range of test Mach numbers that the suction can increase the lift coefficient for some suction quantity range. The lift increment generates a higher L/D value than that expected from the drag reduction alone and gives a favorable effect to the HLFC technology. These results seem to support our design concept of suction hole arrangement. The present HLFC wing has no three-dimensional aerodynamic design including suction effect and thus the test of a wing with such design will be a

next study item.

Acknowledgment

The authors wish to thank Seigo Nakamura, Akira Koike and Nobuyuki Hosoe of the Aerodynamic Division for their helpful assistance during the wind tunnel test and Kenji Yoshida of the Advanced Technology Aircraft Project Center for stimulating discussions.

REFERENCES

- 1) O. Nonaka, Y. Ishida, M. Sato, and H. Kanda, "An Investigation of a Two-Dimensional Hybrid Laminar Flow Control Airfoil at High Subsonic Flow, Part 1: Aerodynamic Characteristics of a Basic Airfoil NLAM78" (In Japanese) National Aerospace Laboratory TR-1076 (1990).
- 2) M. Noguchi, M. Sato, H. Kanda and Y. Ishida, "High Subsonic and High Reynolds Number Wind Tunnel Tests of Two-Dimensional Natural-Laminar-Flow Airfoil with Suction Boundary Layer Control" (In Japanese) National Aerospace Laboratory TR-1204 (1993).
- 3) J.N. Hefner, "Laminar Flow Control: Introduction and Overview", In *Natural Laminar Flow and Laminar Flow Control* (ed. R.W. Barnwell and M.Y. Hussaini), Springer-Verlag, New-York (1992), pp. 1-21.
- 4) Boeing Commercial Airplane Company, "F-111 Natural Laminar Flow Glove Flight Test Data Analysis and Boundary-Layer Stability Analysis", NASA CR-166051 (1984).
- 5) R.D. Wagner, D.V. Maddalon, D.W. Bartlett, F.S. Collier and A.L. Braslow, "Laminar Flow Flight Experiments — Review" In *Natural Laminar Flow and Laminar Flow Control* (ed. R.W. Barnwell and M.Y. Hussaini), Springer-Verlag, New-York (1992), pp. 23-71.
- 6) W. Nitsche and J. Szodruch, "Concepts and Results for Laminar Flow Research in Wind Tunnel and Flight Experiments", ICAS-90-6.1.4, Sep. 1990.
- 7) Y. Ishida, M. Noguchi, M. Sato and H. Kanda, "Numerical and experimental study of drag characteristics of two-dimensional HLFC

- airfoils in high subsonic, high Reynolds number flow", National Aerospace Laboratory TR-1244T (1994).
- 8) C.W. Brooks, Jr., C.D. Harris and W.D. Harver, "The NASA Langley Laminar-Flow-Control Experiment on a swept, Supercritical Airfoil — Drag Equations" NASA Tech.Memo. 4096, (1989).
 - 9) Y. Ishida, M. Noguchi, S. Kayaba, O. Nonaka and H. Hoshino, "An Experimental Study of a Three-Dimensional Swept-Back Wing with Suction Laminar-Flow-Control (In Japanese)" National Aerospace Laboratory TR-1072 (1990).
 - 10) F.S. Colliar, Jr, "An overview of recent subsonic laminar flow control flight experiments" AIAA Paper 93-2987 (1993).
 - 11) P.K. Bhutiani, D.F. Keck, D.J. Lahti and M.J. Stringas, "Investigating the merits of a hybrid laminar flow nacelle". *The Leading Edge, Gen. Electric Co Rep., Spring*, pp. 32-35 (1993).
 - 12) J. Reneaux and A. Blanchar, "The design and testing of an airfoil with hybrid laminar flow control". *Proc. Eur. Forum Laminar Flow Tech, 1st. Hamburg*, pp. 164-74. Bonn, Germany: DGLR (1992).
 - 13) B. Barry, S.J. Peak, N.W. Brown, H. Riedel and M. Sitzmann, "The flight testing of natural and hybrid laminar flow nacelles". ASME 94-GT-408 (1994).
 - 14) D.W. Holder, D.C. Macphail and J.S. Thompson, "Experimental Methods", In *Modern developments in fluid dynamics: High speed flow vol. II (ed. L. Howarth)* p. 565 (1953).